Available online at www.sciencedirect.com

ScienceDirect

International Journal of Heat and Mass Transfer 51 (2008) 1913–1919

International Journal of HEAT and MASS TRANSFER

www.elsevier.com/locate/ijhmt

Flow boiling CHF enhancement with surfactant solutions under atmospheric pressure

Yong Hoon Jeong *, Mohammad Sohail Sarwar, Soon Heung Chang

Korea Advanced Institute of Science and Technology, 373-1, Guseong-dong, Yuseong-gu, Daejeon 305-701, Republic of Korea

Received 12 December 2006; received in revised form 17 June 2007
Available online 25 September 2007

Abstract

Surfactant effect on CHF (critical heat flux) was determined during water flow boiling at atmospheric pressure in closed loop filled with solution of tri-sodium phosphate (TSP, $Na_3PO_4 \cdot 12H_2O$). TSP was added to the containment sump water to adjust pH level during accident in nuclear power plants. CHF was measured for four different water surfactant solutions in vertical tubes, at different mass fluxes (100–500 kg/m^2 s) and two inlet subcooling temperatures (50 °C and 75 °C). Surfactant solutions (0.05–0.2%) at low mass flux (~100 kg/m^2 s) showed the best CHF enhancement. CHF was decreased at high mass flux (500 kg/m^2 s) compared to the reference plain water data. Maximum increase in CHF was about 48% as compared to the reference data. Surfactant caused a decrease in contact angle associated with an increase of CHF from surfactant addition.

Keywords: Flow boiling; Surfactant; CHF; Wettability

1. Introduction

Critical heat flux (CHF) defines the upper limit for safe operation of heat transfer equipment in heat flux controlled systems. In nuclear power plants, insufficient cooling during an overpower transient or a loss of coolant accident may cause CHF leading to core meltdown and subsequent release of radioactive material into the environment [1].

The most common technique to suppress iodine volatility in nuclear power plants (NPP's) is to maintain a high pH in water within reactor containment. High pH converts molecular iodine into a nonvolatile form and suppresses the formation of organic iodides. The requirement to maintain a high pH imposes design requirements during normal operation and following accidents. Spray systems are used to suppress release of airborne iodine from breathing of paints on containment surfaces. Sprays are effective if spray water contains low concentrations of volatile forms of iodine. Sodium hydroxide (NaOH), lithium hydroxide (LiOH), boric acid, hydrazine and TSP ($Na_3PO_4 \cdot 12H_2O$) are used to control pH in spray water [2].

Some additives enhance heat transfer, although, the magnitude and mechanism of enhancement are not consistent or clearly understood. The surfactant concentrations are usually low enough that, the addition of surfactant to water causes no significant change in saturation temperature and most other physical properties, except viscosity and surface tension. A low concentration of surfactant is effective in reducing surface tension. Surface tension will influences the activation of nucleation sites, bubble growth and dynamics, affecting the boiling heat transfer coefficient [3,4].

Frost and Kippenhan [5] attributed increased CHF to the inhibition of vapor bubble coalescence over the boiling surface by the Marangoni effect, which is a result of slowness of surfactant migration from the bulk to the adsorption layer at the extending vapor/liquid interface during bubble coalescence. A small amount of surfactant can increase boiling heat transfer. The extent of CHF enhancement is dependent on additive concentrations, its type and chemistry, wall heat flux, and heater geometry [6]. Although many

* Corresponding author. Tel.: +82 42 869 3891; fax: +82 42 869 3810.
E-mail addresses: jeongyh@kaist.ac.kr (Y.H. Jeong), sohail@kaist.ac.kr (M.S. Sarwar), shchang@kaist.ac.kr (S.H. Chang).

0017-9310/$ - see front matter © 2007 Elsevier Ltd. All rights reserved.
doi:10.1016/j.ijheatmasstransfer.2007.06.044

Nomenclature

A	ampere
A	flow area (m^2)
D	tube diameter (m)
G	mass flux (kg/m^2 s)
h	heat transfer coefficient (W/m^2 s)
h_{fg}	latent heat of vaporization
k	thermal conductivity (W/m K)
k	wave number (m^{-1})
L	length of a heated tube (m)
L	characteristic length (m)
q	heat flux (kW/m^2)
R	resistance (ohm)
Re	Reynolds number
U	velocity (m/s)
V	volt (V)
We	Weber number

Greek symbols

μ	dynamic viscosity (N s/m^2)
λ	wave length (m)
ρ	specific resistance (Ω m)
ρ	density (kg/m^3)
ρ_c	density of liquid droplets (kg/m^3)
σ	surface tension (N/m)
τ	shear stress

Subscripts

g	gas
i	interface
TSP	TSP solution
water	pure water

investigators have conducted experiments to determine the boiling enhancement mechanisms caused by addition of surfactants to water, the effects of surfactant on boiling heat transfer are still unclear [3–7]. The main concern remained the decrease in surface tension and increase in viscosity.

Hetsroni et al. [7] found that heat transfer coefficient depends both on the surface tension and the kinematic viscosity. The increase of the heat transfer coefficient at a low surfactant concentration was attributed to decreasing surface tension, while at a high concentration, the increase in kinematic viscosity decreased the heat transfer coefficient. Many studies have shown the importance of surface tension decreased by adding additives on the boiling heat transfer coefficient. Wu et al. [8] have studied the effects of surface tension on surfactant boiling with various concentrations of surfactants.

This study examines water flow boiling CHF enhancement with tri-sodium phosphate TSP ($Na_3PO_4 \cdot 12H_2O$) surfactant added in the water loop at four concentrations (0.05%, 0.2%, 0.5% and 0.8%). Studies were performed at atmospheric pressure, at a mass flux of 100–500 kg/m^2 s and at an inlet subcooling temperature of 50–75 °C. Results were compared with reference plain water CHF data. Wettability was determined by measuring the contact angle at different concentration cases that will substantiate any CHF increase.

2. Experimental apparatus and procedure

2.1. Experimental loop

The flow boiling heat transfer experiment was performed using the low pressure water CHF test loop at the Korea Advanced Institute of Science and Technology (KAIST). In a closed water flow boiling loop, a test section was directly heated using an electrical DC power supply unit. The schematic diagrams of test loop and tubular test section are shown in Figs. 1 and 2. The experiments were carried out at atmospheric pressure by venting to ambient. The main test loop consisted of a condenser, surge tank (with overhead water reservoir), a centrifugal pump, turbine flow meter, two pre-heaters (to control the inlet water temperature and subcooling), needle valve (to provide throttling) and a test section. Filtered water or TSP solutions filled the loop.

Thermocouples, pressure transducers, flow transducers and other instrumentations were connected to a HP

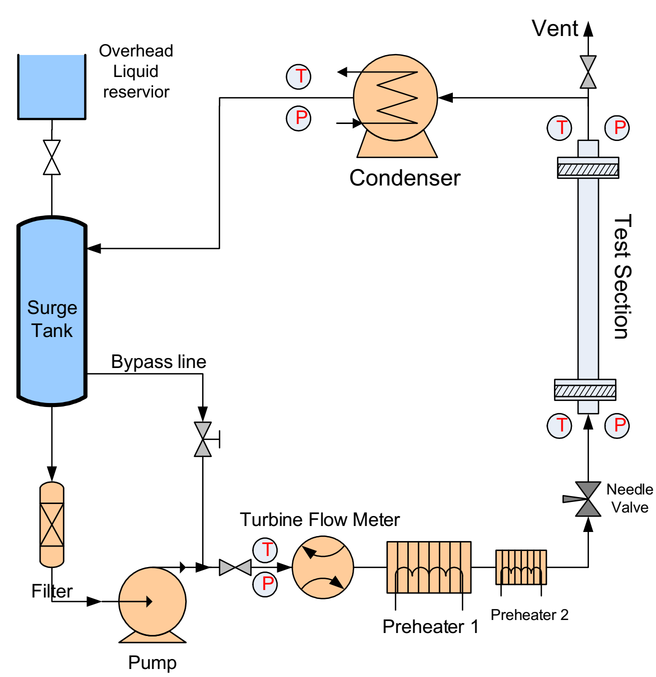

Fig. 1. Schematic diagram of experimental test loop. (T) Temperature measurement and (P) pressure measurement.

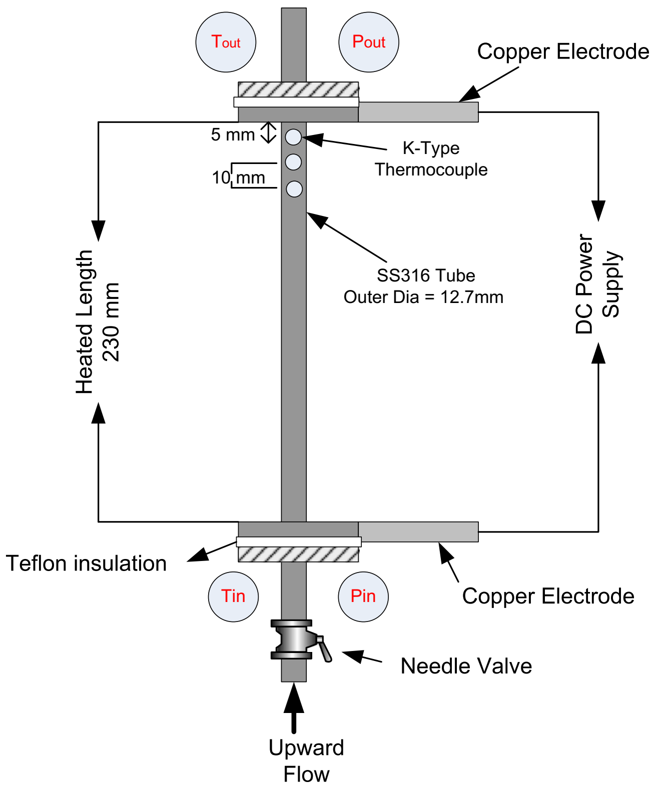

Fig. 2. Schematic diagram of the test section.

3852A data acquisition/control unit for data collection and processing.

2.2. Test section

Water flows in an upward direction in the test section tube. The dimensions of the cylindrical tube and flow parameters are listed in Table 1. The test section was made of SS-316 circular tube of 12.7 mm outer diameter and 230 mm length. Three Type-K thermocouples (outer diameter = 1.5 mm) were attached onto the outer surface of the test section to measure wall temperature and detect onset of CHF. The first thermocouple was located at 5 mm below the top of the heated tube. The distance between each thermocouple was 10 mm. Copper electrodes were connected to the both end of the heated length. The tube between top and bottom electrodes was heated by Joule heating with a DC power transformer with a maximum capacity of 32 V and 2000 A. The test section was connected to the flange, which was insulated from rest of the part of the test loop by Teflon. The current and voltage difference between both electrodes were measured. The temperatures of the water at the inlet and outlet of the test section were measured with in-stream T-type sheathed thermocouples. Outlet pressure and inlet pressure were measured with pressure transducers and calibrated to 0.5% of RMS error for a full range.

Table 1
Test matrix

	Parameters
Uniformly heated vertical cylindrical tube	
Geometry	
Outer diameter	12.7 mm
Inner diameter	10.92 mm
Heated length	230 mm
Vertical upward flow	
Flow	
Pressure	101.3 kPa (1 atm)
Mass flux	100–500 kg/m^2 s
Inlet subcooling	50–75 °C

2.3. Test procedure

CHF data was taken for all test conditions shown in Table 1. The experimental loop was filled with water or TSP solutions, which were heated in the loop by preheaters in order to remove non-condensable gas. Degassing was conducted at atmospheric pressure, with opening of vent valves on top of the surge tank and preheaters, and stopped when gas was not detected in the venting line. Heat balance tests performed before each series of experiments showed heat losses to be <2%. Entering water temperature in the test section was kept constant by electronically controlled preheaters in series. Flow rate was measured by a turbine flow meter (Omega FTB 505 VDC, 0.2–2.0 gal/min), and mass flux was calculated in real time.

During the measurements, the heating power in the test section was gradually increased by slowly increasing the voltage. The heat flux increment used near the CHF was ~10 kW/m^2. The voltage of the test section increased step by step with sufficient time for thermal equilibrium of the working fluid in the loop and stabilization of the loop. At least two consecutive runs were conducted for each condition. CHF condition was defined as a sudden increase in the temperature (~50 °C) of the tube surface. CHF onset position was the point where the first wall temperature jump took place. At that moment, power to the test section was immediately switched off to avoid damage to the heated surface. Heat flux was calculated from applied voltage and current. CHF experiments were performed at two inlet subcooling temperatures (50 °C and 75 °C) and four mass flux levels (100, 200, 300 and 500 kg/m^2 s) (Table 1).

2.4. TSP solution

Tri-sodium phosphate TSP ($Na_3PO_4 \cdot 12H_2O$) surfactant was added to the spray system or sump water for maintaining high pH level during accidents.

In order to find the optimized concentration of surfactant water solution, the CHF experiment was performed with four different concentrations:

(i) 0.05% solution,
(ii) 0.2% solution,
(iii) 0.5% solution,
(iv) 0.8% solution.

TSP solution was filled in the closed loop to perform CHF flow boiling experiment.

2.5. Uncertainty analysis

Uncertainty analyses were estimated by the method of Moffat [9]. Mass flux uncertainty was estimated as ~5% at 100 and 200 kg/m^2 s and ~3% at 300 and 500 kg/m^2 s. Uncertainty in pressure measurements were estimated as 3%. To avoid any measurement variation error between the three test section thermocouples, a test run was performed for each heater. The temperature measurement uncertainties were primarily estimated considering the thermocouple calibration and temperature correction from the thermocouple reading to the reference surface. The maximum variation of three measured wall temperatures (K-type thermocouples) was ±0.5 °C. The uncertainty in the inlet and outlet water temperatures (T-type thermocouples) was estimated to <±1 °C. The maximum error in controlling inlet subcooling temperature was ±2 °C.

Uncertainty in heat flux was observed by taking into account voltage and electrical resistance ($R = \rho\frac{L}{A}$) uncertainties, where ρ is resistivity and L and A are length and flow area, respectively. To estimate heat loss to external surroundings, conservative calculations were performed at various heat flux conditions for the heated test section geometry. Heat losses were calculated at different heat flux conditions with the help of computer code (FLUENT 6.0). Heat losses to the surroundings were less than 1.0% for heat flux conditions of 100–900 kW/m^2 assuming a uniform temperature distribution with heater surface temperature of 180 °C. Heated surface area also contributed to the uncertainty. Considering all these factors, the overall uncertainty of heat flux was ~4%. Taking in to account the uncertainties of heat flux and power, the uncertainty in CHF was 5%.

2.6. Wettability and contact angle measurement

The extent to which the liquid phase spreads over the solid phase is called wettability. The wettability of a solid by a liquid is characterized in terms of the angle of contact that the liquid makes with a solid. The hydrophilicity of the liquid phase was investigated through changes in contact angle.

A water and surfactant solution drop test was performed to check the wettability of fluids and to measure the contact angle. Water was dropped on a dry surface strip (area = 1 cm^2). A high contact angle meant decreased wettability or less hydrophilicity. Surfactant causes a decrease in contact angle due to increased hydrophilicity (Fig. 3).

3. Results and discussion

All experiments were performed in flow boiling water at atmospheric pressure in fixed inlet conditions of temperature and mass flux. The linear trend of CHF as function of mass flux (100–500 kg/m^2 s) is shown at inlet subcooling temperatures of 50 °C and 75 °C (Fig. 4). The maximum

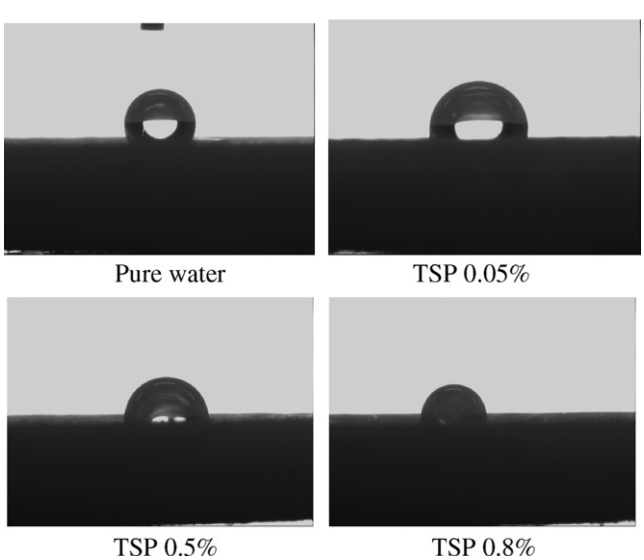

Fig. 3. Contact angle measurement for water and surfactant solutions drop on Teflon strip.

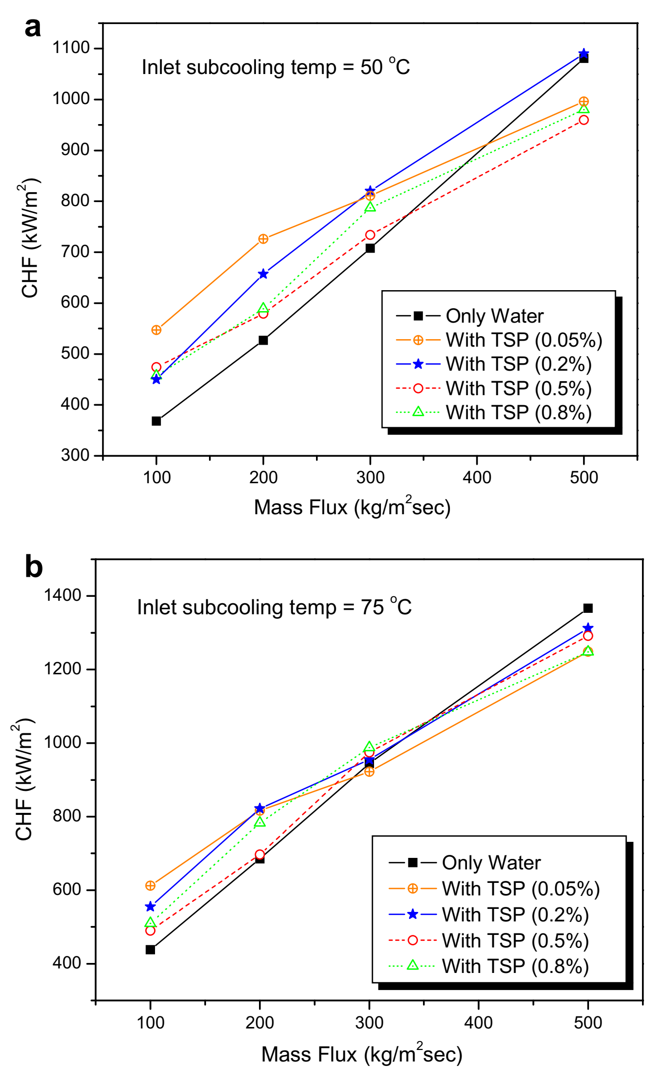

Fig. 4. CHF as a function of mass flux for water and for different concentrations of surfactant for inlet subcooling temperatures of 50 °C (a) and 75 °C (b).

increase in CHF was observed at very low mass flux (100 kg/m^2 s) as compared to higher mass fluxes. A maximum increase in CHF (∼48%) was observed with 0.05% TSP water solution at an inlet subcooling temperature of 50 °C. CHF enhancement was lowered as the mass flux increased (200–300 kg/m^2 s), while some decrease in CHF (∼8%) was observed with surfactants at higher mass flux (500 kg/m^2 s), as compared to plain water data. At 50 °C inlet subcooling temperature, the CHF enhancement was more pronounced as compared to high inlet subcooling (75 °C). Increase of CHF by adding TSP in water at low mass flux (∼150 kg/m^2 s) was also observed in Jeong et al. [10] large scale experiments which simulated an external reactor vessel cooling.

Using the plot of Hewitt and Roberts [11] for vertical upward flow, flow patterns were explored at different mass flux levels (Fig. 5). At low mass flux (100–300 kg/m^2 s) the flow patterns were slug-churn, while for relatively high mass flux (∼500 kg/m^2 s) the flow pattern was in bubbly–slug region. The critical quality as a function of mass flux at inlet subcooling temperatures of 50 °C and 75 °C is shown in Fig. 6. The addition of TSP helped to increase the wettability by reducing the surface tension. This happens with the decrease in bubble diameter, breakup of bubbles and avoidance of bubble coalescence. Thus, surfactant enhances the CHF as compared to plain water data. At relatively high mass flux (500 kg/m^2 s), the flow regime was bubbly–slug (Fig. 5). The reduced surface tension due to addition of TSP caused a decrease in the stabilizing force of large slugs. CHF increase or decrease depends upon competition between high wettability (at low mass flux) and high instability (at relatively high mass flux). The unstable and wavy slugs resulted in the decrease of CHF under the circumstances described in Fig. 7. High degree of subcooling (50–75 °C), very low quality and low L/D (∼20) also contributed in high instability (Kelvin–Helmhotz) as the mass flux increases (∼500 kg/m^2 s). Therefore, based upon the critical quality results (Fig. 6), we can infer that CHF increases with TSP solutions for saturated flow boiling and CHF decreased with TSP solutions for subcooled flow boiling. Under subcooled flow boiling condition, for low quality CHF (DNB type), Celata et al. [12] and Chang et al. [13] supported the liquid sublayer dryout model. Chang et al. [13] demonstrated the existence of continuous liquid sublayer under coalesced bubbles (or slugs). The experimental data is not covering for higher qualities, where the annular flow regime follows the deposition/entrainment controlled annular film dryout.

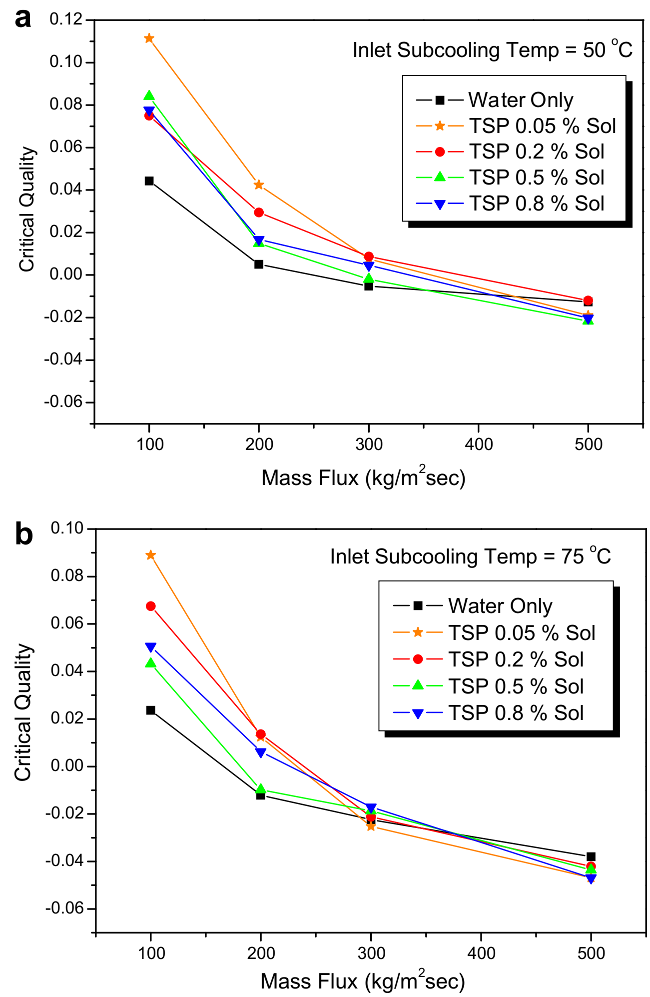

Fig. 6. Critical quality as a function of mass flux at inlet subcooling temperature of 50 °C (a) and 75 °C (b).

The main difference in physical properties of plain water and TSP solution is surface tension [3–7]. TSP is popular ingredient of detergent for general use such as dish washing. TSP lowers the surface tension of water increasing wettability. At high concentrations of TSP (more than several percent), viscosity and density are significantly changed. At low concentrations of TSP (<1%), a reduced surface tension is the major difference compared to the plain water. Thus, reduced surface tension results in better wettability and shorter wave length on the interface between liquid and vapor.

Significant decrease in contact angle was observed with surfactant solution as compared to pure water (Fig. 3).

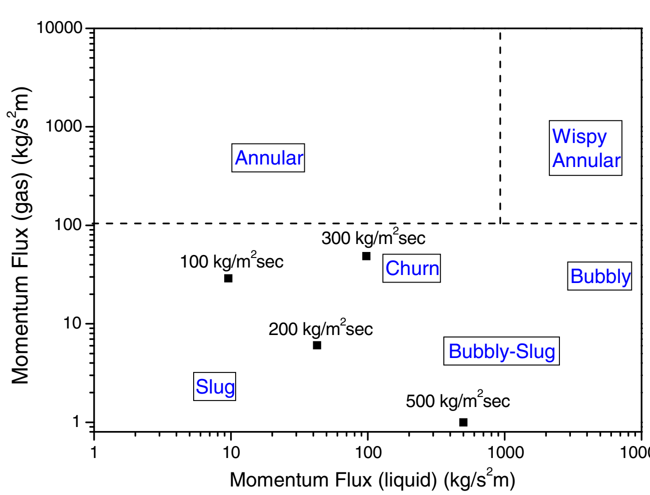

Fig. 5. Flow patterns on the basis of Hewitt and Roberts [11] map.

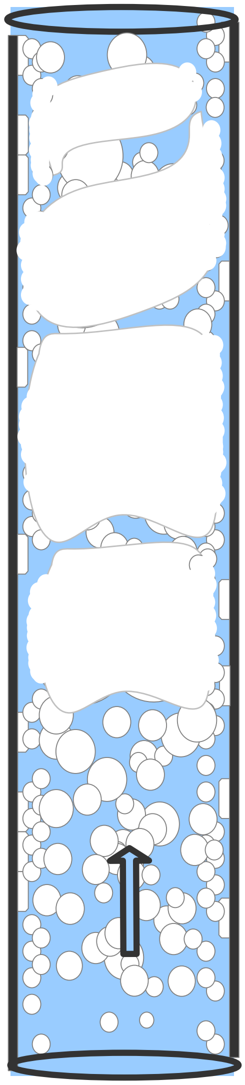

Fig. 7. CHF mechanism with TSP.

This helped to elaborate the boiling experimental results, because decreased contact angle is a measure of wettability. The surface tension of each solution was estimated by the relationship between solid surface tension and liquid surface tension, using measured contact angle of the drop of water on smooth Teflon FEP surface. Using the known solid surface tension, liquid surface tension was calculated by the measured contact angle [14]. The measured surface tension of pure water and TSP solutions are shown in Fig. 8. Surface tension was decreased by addition of TSP in water. The 0.5% TSP showed the lowest surface tension at 25 °C. Under boiling condition (∼100 °C), the surface tension may decrease from its value at room temperature. For water, surface tension decreases from 72 mN/m to 59 mN/m.

CHF enhancement under low mass flux and slug or churn flows can be a result of enhanced wettability (decreased contact angle) by TSP. The decrease in surface tension helps in bubble breakup which leads to more nucleate boiling and increased CHF. However, decreased CHF

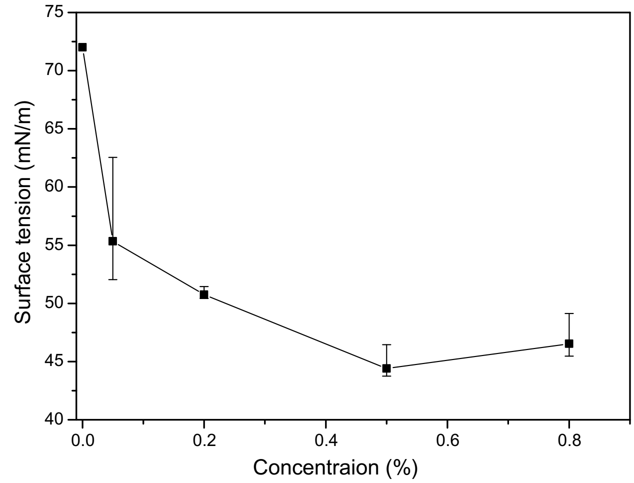

Fig. 8. Surface tension of pure water and TSP solutions at a temperature of 25 °C.

under high mass flux and bubbly–slug flow can be explained by flow instability.

Kelvin–Helmholtz (KH) flow instability results from velocity shears between two fluids. Any time there is a non-zero curvature, the flow of one fluid around another will lead to a slight centrifugal force which in turn leads to a change in pressure thereby amplifying the ripple. The most familiar example of this is wind blowing over calm water. Tiny dimples in the smooth surface will quickly be amplified to small waves. Surface tension will hinder KH instabilities. If there is some restoring force, surface tension (σ), the instability of horizontal flow will arise [15], if:

$$\Delta U^2 \geqslant \frac{(\rho_g + \rho_f)}{\rho_g \rho_f}\left[k\sigma + \frac{g}{k}(\rho_f - \rho_g)\right]$$

where ΔU is the velocity difference between two-phases and k is wave number.

Gravity force and surface tension play a role as stabilizer in horizontal flow. However, for vertical flow, the surface tension is the only stabilizing force. Therefore, for the reduced surface tension, a reduced critical velocity can be expected above which the liquid film on the heated wall can be broken by instability.

The Weber number is a dimensionless number that is useful in analyzing fluid flows where there is an interface between two different fluids. It can be thought of as a measure of the relative importance of the fluid's inertia compared to its surface tension. The quantity is useful in analyzing thin film flows and formation of droplets and bubbles. It may be written as

$$We = \frac{\rho_g L U_g^2}{\sigma}$$

where ρ_g is the density of the fluid, U_g is its velocity, L is its characteristic length, and σ is the surface tension. The characteristic length can be written as

$$L = \frac{\lambda}{2}$$

where λ is wave length of liquid film on the heated wall.

The Weber number can be re-written as

$$We = \frac{\rho_g \lambda U_g^2}{2\sigma}$$

The critical Weber number for droplet breakup is given by Duan et al. [16]:

$$We_{cr} = 4\pi\left(1 + \frac{\rho_g}{\rho_f}\right)$$

For steam–water system under atmospheric conditions, the critical Weber number is 12.6. For a given critical Weber number, the critical steam velocity is reduced as the surface tension force is reduced. Therefore, the CHF could be reduced by reduced surface tension.

Aging process may modify structures of surfactants and its performance may affected with time and temperature increase. The surface tension of aqueous surfactant solutions are temp dependent because the particles become more compact with time. An optimum surfactant concentration is needed which must have high crystalline content. The concentration of the solutions has a great effect on the surface tension of the solutions. When the concentration reaches at a critical value, the surface tension will tend to a constant value which corresponds to the critical micelle concentration (cmc) for each surfactant. In addition, the surface tension of the aqueous surfactant solutions has also been found to be temperature dependent. Zhang and Manglik [17] compared the variation of equilibrium surface tensions of various surfactant solutions and water with temperature.

4. Conclusions

Subcooled flow boiling CHF with SS316 tubes at atmospheric pressure was studied. Significant findings were:

(1) Surfactant solutions showed decrease in contact angle, means high wettability and low surface tension.
(2) Enhanced (~48%) CHF was observed for surfactant (TSP) solution under low mass flux (100–300 $kg/m^2 s$). CHF enhancement was more pronounced at very low mass flux (~100 $kg/m^2 s$), which is due to an increasing wettability of the heater surface and promoted liquid supply under bubbly or churn flow conditions.
(3) CHF decreased at high mass flux (500 $kg/m^2 s$), which is due to instability of liquid slug flow condition by reduced surface tension.

Acknowledgement

This work was sponsored by the Korean Ministry of Science and Technology.

References

[1] S.G. Kandlikar, Critical heat flux in subcooled flow boiling – an assessment of current understanding and future directions for research, Multiphase Sci. Technol. 13 (32) (2001) 207–232.
[2] Nuclear Energy Agency (NEA), Insights into the control of the release of iodine, cesium, strontium and other fission products in the containment by severe accident management, NEA/CSNI/R, 2000.
[3] G. Hetsroni, M. Gurevich, A. Mosyak, R. Rosenblit, Z. Segal, Boiling enhancement with environmentally acceptable surfactant, Int. J. Heat Fluid Flow 25 (2004) 841–848.
[4] D.S. Wen, B.X. Wang, Effects of surface wettability on nucleate pool boiling heat transfer for surfactant solutions, Int. J. Heat Mass Transfer 45 (2002) 1739–1747.
[5] Walter Frost, Charles J. Klppenhan, Bubble growth and heat-transfer mechanisms in the forced convection boiling of water containing a surface active agent, Int. J. Heat Mass Transfer 10 (1967) 931–949.
[6] V.M. Wasekar, R.M. Manglik, A review of enhanced heat transfer in nucleate pool boiling of aqueous surfactant and polymeric solutions, J. Enhanced Heat Transfer 6 (1999) 135–150.
[7] G. Hetsroni, M. Gurevich, A. Mosyak, R. Rozenblit, L.P. Yarin, Subcooled boiling of surfactant solutions, Int. J. Multiphase Flow 28 (2002) 347–361.
[8] Wuu-Tsann Wu, Horng-Shyang Lin, Yu-Min Yang, Jer-Ru Maa, Critical heat flux in pool boiling of aqueous surfactant solutions as determined by the quenching method, Int. J. Heat Mass Transfer 37 (15) (1994) 2377–2379.
[9] Robert J. Moffat, Describing the uncertainties in experimental results, Exp. Therm. Fluid Sci. 1 (1988) 3–17.
[10] Yong Hoon Jeong, Soon Heung Chang, Won-Pil Baek, Critical heat flux experiments on the reactor vessel wall using 2-d slice test section, Nucl. Technol. 152 (2) (2005) 162–169.
[11] G.F. Hewitt, D.N. Roberts, Studies of two-phase flow pattern by simultaneous X-ray and flash photography, UKAEA Report AERE-M 2159.
[12] G.P. Celata et al., Preliminary remarks visualization of high heat flux burnout in subcooled water flow boiling, Two Phase Flow Model. Exp. 859 (1995).
[13] S.H. Chang, I.C. Bang, W.P. Baek, A photographic study on the near-wall, bubble behavior in subcooled flow boiling, Int. J. Therm. Sci. 41 (2002) 609–618.
[14] D.Y. Kwok, A.W. Neumann, Contact angle interpretation in terms of solid surface tension, Colloids Surfaces A 161 (2000) 31–48.
[15] D.J. Acheson, Elementary Fluid Dynamics, Clarendon Press, Oxford, 1990.
[16] Ri-Qiang Duan, Seiichi Koshizuka, Yoshiaki Oka, Numerical and theoretical investigation of effect of density ratio on the critical weber number of droplet breakup, J. Nucl. Sci. Technol. 40 (7) (2003) 501–508.
[17] J. Zhang, R.M. Manglik, Effect of ethoxylation and molecular weight of cationic surfactants on nucleate boiling in aqueous solutions, J. Heat Transfer 126 (2004) 34–42.